DRDC Ottawa SL 2003-130

SURVEILLANCE THROUGH CONCRETE WALLS

Sylvain Gauthier*, Radar Systems Section
Walid Chamma, Radar Electronic Warfare Section
Defence R&D Canada – Ottawa, 3701 Carling Avenue, Ottawa, Ontario, K1A 0Z4

ABSTRACT

This paper studies the capability of ultra-wideband short-pulse (UWB SP) radar to provide surveillance through concrete walls, including multistatic radar surveillance and 3D through-wall imaging. A full-wave electromagnetic simulator is used to generate high fidelity through-wall radar data. The raw radar data are transformed into radar images using a back projection algorithm. It is shown that UWB SP radar can track targets moving inside a room with concrete walls as well as providing static mapping of the room interior. The velocity of the electromagnetic wave inside a concrete wall is reduced compared to free space thus defocusing target images, displacing targets from their true positions, and possibly producing false targets. This problem can be mitigated by including the time of flight difference due to the concrete walls into the image generation algorithm. 3D through-wall radar imaging obtained using UWB SP radar centered at 2 GHz requires a very large antenna aperture to be able to see the shape of the human phantoms. However, using a center frequency of 10 GHz reduces this aperture requirement fivefold making the system more practical operationally. However, attenuation is much higher at 10 GHz than at 2 GHz.

Keywords: Ultra-wideband, radar, through-wall, surveillance, concrete, 3D imaging, multistatic, short-pulses, electromagnetic

1. INTRODUCTION

This paper studies the feasibility of using UWB SP radar to provide surveillance through concrete walls. Buildings with concrete or brick walls are very common throughout the world and are the most likely type of building to be encountered by law enforcement personnel when performing operations in urban terrain [1]. By definition, ultra-wideband (UWB) radars have a relative bandwidth of 25% of the center frequency or larger [2]. There are different types of UWB radars: frequency modulated, step frequency modulated, and short pulse. Typical UWB short pulse (UWB SP) radars transmit pulses with duration from 0.1 nanosecond to a few nanoseconds.

For this study, a full-wave electromagnetic simulator is used to generate high fidelity through-wall radar data. This software is based on the finite-difference time-domain (FDTD) method [3], which is a direct solution of the time-dependent Maxwell's equations using the finite-difference technique. It is analogous to the finite-difference solution of fluid flow problems encountered in computational aerodynamics, where a numerical model is based on a direct solution of the corresponding partial differential equations. In FDTD, the propagation of an EM wave in a volume of space containing a dielectric or a conducting structure (or a combination of both) is modeled. By time stepping, the incident wave transmitted from an antenna is tracked as it first propagates to the structure and then interacts with the latter through current excitation, scattering, multiple scattering, penetration and diffraction.

These simulated through-wall radar echoes are transformed into radar images using a back projection technique that consists of adding each receiver range return onto a spatial grid [5, 6]. The same algorithm is used to produce radar images of static objects as well as moving targets. For the moving targets, however, clutter from fixed objects is removed from the received signals by subtracting the received signals from the received responses of an empty room. Signal propagation in the concrete wall will alter the total return time of the signal, which causes defocusing of the radar images. Section 2 describes how to calculate and compensate for this time difference with the back projection algorithm.

* sylvain.gauthier@drdc-rddc.gc.gc.ca; ph. 1 613 990-7553, walid.Chamma@drdc-rddc.gc.ca; ph 1 613 993-5440

Sensors, and Command, Control, Communications, and Intelligence (C3I) Technologies for Homeland Security and Homeland Defense III, E. M. Carapezza, ed., Proc. of SPIE Vol. 5403 (SPIE, Bellingham, WA, 2004) · 0277-786X/04/$15 · doi: 10.1117/12.533691

In the first part of the paper, UWB SP radar positioned in front of a concrete room having two metallic boxes moving in discrete steps inside the room has been modeled by the electromagnetic group at DRDC Ottawa. This setup has been used to evaluate the capability of UWB SP radar to track moving boxes, as well as providing static mapping of the room layout. The UWB SP radar under study includes a multistatic radar configuration, which is of interest for potential covert surveillance. The second part of the study, models UWB SP 2D antenna array positioned in front of a room with concrete walls. A human phantom, with and without a rifle, is located inside the room. 3D through-wall radar images of the phantoms are obtained using UWB SP radar centered on two different frequencies. Features of these images are discussed below.

2. TRACKING AND MAPPING

2.1.1. Modeling and image processing

Electromagnetic modeling software is used to generate simulated data of an UWB SP radar positioned in front of a concrete room with two moving targets inside. Figure 1 shows the plan view of the concrete room and the two conducting cubes inside the room. The external dimensions of the room are 2.47 m in width, 3.7 m in length and 2.75 m in height. The room floor, ceiling and walls are all made of concrete. The conductivity and relative permittivity of the concrete walls have been set to a standard value of 0.05 S/m and 7 respectively [4]. By definition, the relative permittivity has no units. The UWB SP radar is modeled as a single transmitting antenna consisting of a 9 cm vertical dipole located 1 m above ground and 11 cm in front of the concrete room. The dipole antenna is driven by a 0.6 ns gaussian pulse modulated by a 2 GHz sine wave [4]. The electromagnetic field was recorded every 2 cm around the room to simulate receive signals. This approach gives us the flexibility of studying a receiving array of different sizes, antenna spacing and at various locations. The dimensions of the two metallic cubes are 10x10x10 cm^3 and 30x30x30 cm^3. Thirty different positions of the two boxes have been modeled to simulate targets in motion. For each box position, the radar dipole antenna transmits an UWB SP signal and the reflected echoes are recorded. Table 1 provides the coordinates of the boxes for the positions given in this paper.

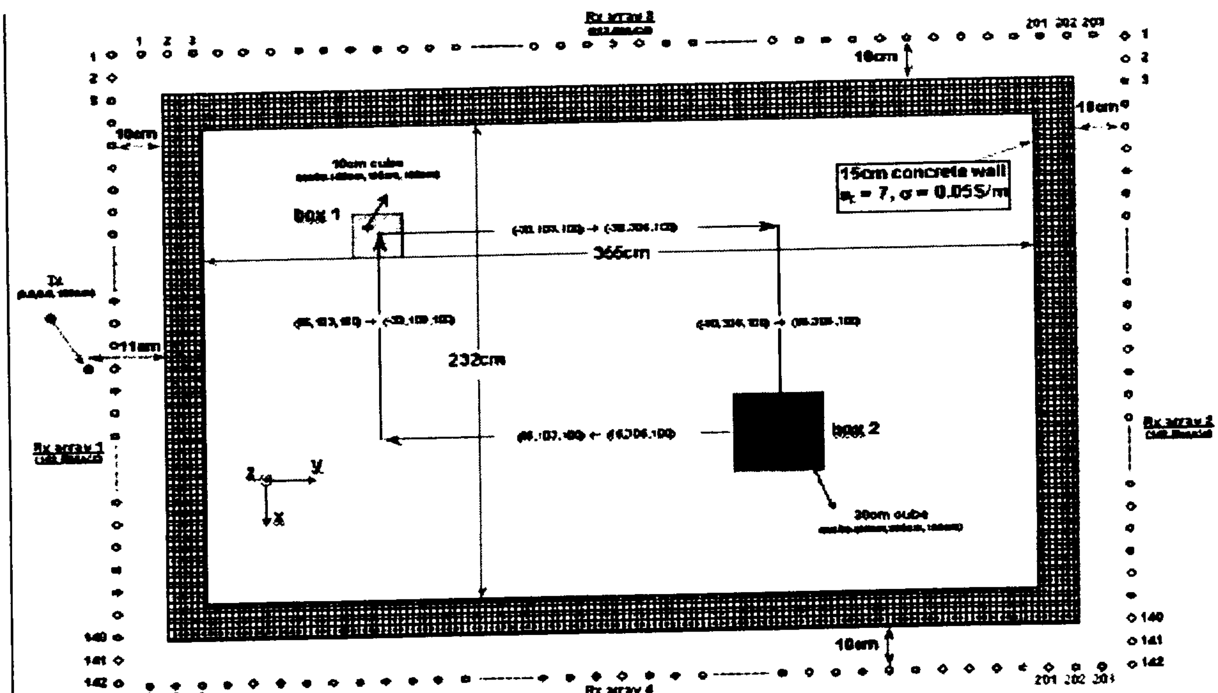

Figure 1. Top view of simulated concrete room scenario

Table 1. Coordinates for each position number for each box

	SMALL BOX		LARGE BOX	
Position	***X centre (m)***	***Y centre (m)***	***X centre (m)***	***Y centre (m)***
1	-0.30	1.03	0.65	3.06
5	-0.30	1.43	0.65	2.66
6	-0.30	1.53	0.65	2.56
10	-0.30	1.93	0.65	2.16
15	-0.30	2.43	0.65	1.66
25	0.10	3.06	0.25	1.03

2.2. Back projection algorithm

The data for each received signal represents a set of electric field values as a function of time. The signal received in a given bin at a given time is from all pixel locations where total flight time is equal to this specific time bin. The back projection technique consists of recording the amplitude of each time bin on a spatial grid. All the recorded amplitudes from each channel are then added together on the spatial grid. At the true target locations the signal amplitudes will add coherently. Mathematically, in free space, the back projected signal at pixel (x_i, y_i) in the room image plane is given by (see Figure 5):

$$I(x_i, y_i) = \sum_n E[t_i(n), n] \tag{1}$$

where,

$$t_i = (R_{Txi} + R_{Rxi}(n))/c \tag{2}$$

$$R_{Txi} = \sqrt{(x_i - x_T)^2 + (y_i - y_T)^2} \tag{3}$$

$$R_{Rxi}(n) = \sqrt{(x_i - x_R(n))^2 + (y_i - y_R(n))^2} \tag{4}$$

where:

c is the speed of light in free space (m/s);
I is the pixel amplitude in V/m;
t is the time in seconds;
x, and y are the pixel coordinates in meters;
n is the receiver number.

The variable $t_i(n)$ is the total time taken for the transmitted signal to travel from the transmitter to pixel (x_i, y_i) and return to receiver n. R_{Txi} and $R_{Rxi}(n)$ are, respectively, the ranges in meters from the transmitter and receive point n to pixel (x_i, y_i). The set {x_T, y_T} are the coordinates of the transmitter and the set {$x_R(n)$, $y_R(n)$} are the coordinates of the nth receiver. The result of this procedure is a 2D radar image, which displays the position of the potential targets moving behind the walls.

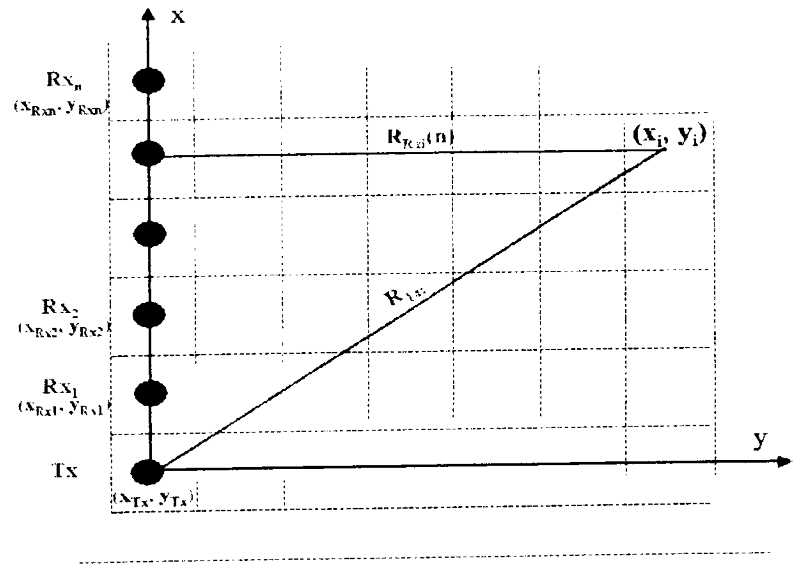

Figure 2. Schema of a Transmitter and Receives points on a spatial grid

The accurate determination of the total flight time is a critical step in the back projection algorithm. The velocity of the signal inside concrete is slower than in free space. This will result in longer flight times for a given set of transmitter, pixel and receiver locations. The time for a radar signal to travel a given distance d_{inwall} inside a wall is given by:

$$t_{inwall} = \frac{d_{inwalll}}{v_{wall}} \tag{5}$$

where v_{wall} is the velocity of the signal inside the wall. For non-magnetic materials such as concrete, the velocity of the electromagnetic signal is given by [6]:

$$v_{wall} = \frac{c}{\sqrt{\varepsilon_{r\_wall}}} \tag{6}$$

where c is the speed of light in free space and ε_{r_wall} is the relative permittivity of the wall. The delay time through concrete compared to free space propagation is then determined by

$$t_{delay} = \frac{d_{inwall}}{c}(\sqrt{\varepsilon_{r\_wall}} - 1) \tag{7}$$

The permittivity of concrete is set to the standard level of seven to generate the simulated data. The wall coordinates are shown in Figure 1. Hence, the travel time difference due to concrete can be included in the back projection algorithm as follows.

$$t_i = \frac{(R_{Txi} + R_{Rxi}(n))}{c} + \frac{d_{inwall}}{c}(\sqrt{\varepsilon_{r\_wall}} - 1) \tag{8}$$

2.2.1. Moving targets

This subsection examines the capability of UWB SP radar to provide radar images of moving targets through concrete walls. By moving targets, one means the isolated targets responses obtained by subtracting the received signals from the empty room response. This process removes the stationary clutter and keeps only changes inside the room. Figure 3 shows radar images of the boxes at position 1 inside the room obtained with and without correction for the slower signal velocity inside concrete. The radar "blobs" represent radar images of the moving targets. The initial positions of the boxes, antenna elements and concrete walls have been superimposed on these figures to emphasize the impact of concrete walls on the radar image. The signal velocity decrease inside the concrete wall has three effects on the radar images. Firstly, the radar target images are displaced from their true positions. Secondly, the target images are significantly defocused as compared to the "no walls" case. Thirdly, the radar images created with concrete walls produce false targets that lie outside of the room. Correcting for signal velocity inside the wall improves considerably the focusing and quality of the radar images, which are comparable in quality to the "no walls" case. These images show that UWB SP radar is capable of tracking targets moving behind a concrete wall.

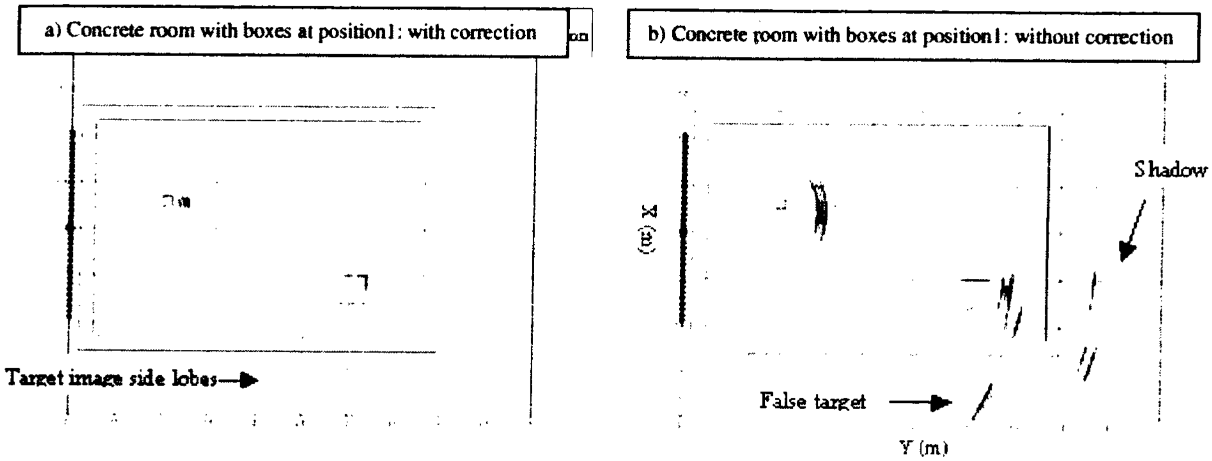

Figure 3. Radar Images of the moving boxes at position 1 with and without correction for signal velocity inside concrete

2.2.2. Static mapping

The radar images in this section were obtained by applying the back projection algorithm directly to the received radar data without any pre-processing. The raw received signals include both the direct coupling to the receive antenna and echoes from the concrete room and the boxes. For this case, the direct signal from the transmit antenna, being much stronger than the other echoes, makes it difficult to see the smaller signals such as wall echoes. Hence, a logarithmic scale has been used to better display the radar images of the targets and the room layout.

Using static mapping, Figure 4 shows the boxes at position 6, with and without correction for the propagation delay of the signal inside the walls. The reflection from the ground and the back wall are visible as well as the coupling between the antennas. The sidewalls are not visible since incident signals are only reflected forward and cannot be seen with the back receiver. In both cases the targets are also clearly visible. With corrected signal velocity, due to propagation inside the walls, the radar images of the targets and back wall are closer to their true positions. The target images are also much better focused. The sidelobes of the back wall and the large box images are no longer parabolic as in free space. This is due to the way in which the wave propagates inside and outside the room. In short, UWB SP radar, as defined here, can be used to provide static mapping of the room layout including fixed targets.

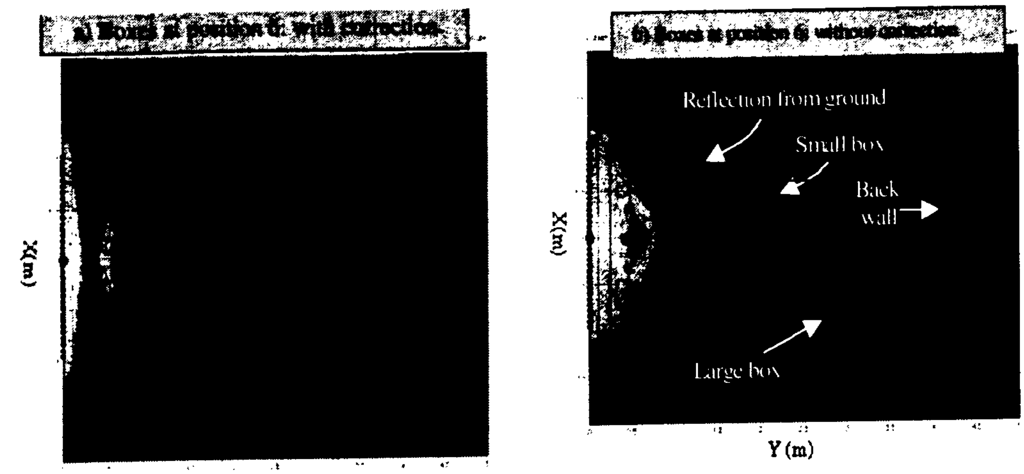

Figure 4. Static mapping of concrete room with and without correction for velocity inside walls

2.2.3. Multistatic through-wall radar surveillance

The best way to study the capability of UWB SP multistatic radar of providing through-wall surveillance is to first examine its capabilities without the presence of walls. Figure 5 shows radar images of the isolated target responses without the presence of concrete walls. Isolated target responses can be obtained by subtracting the received signals with and without the presence of the boxes. The images have been obtained using the same receiver array located at different positions along the sidewall. These positions correspond to a sub-array of "array 4", of Figure 1. In figure 5a the isolated targets responses are clearly visible and localized on the radar image. In figure 5b the radar images do not look as good and are considerably spread in space. A close inspection of the corresponding radar images with static mapping shows that the direct signal is spread along a parabolic curve and is very strong. If the boxes are located within that region then the radar images of the moving boxes will be very spread in space due to the parabolic curve. For moving targets the clutter suppression technique does not work well since the direct coupling is different from the empty room response. As a result, the subtraction with the empty room response will still include a strong contribution from the direct signal. UWB SP multistatic radar works relatively well as long as the targets are not located in the direct coupling region, i.e., as long as the indirect echoes arrive after the direct signal. The same conclusion applies in presence of the concrete walls.

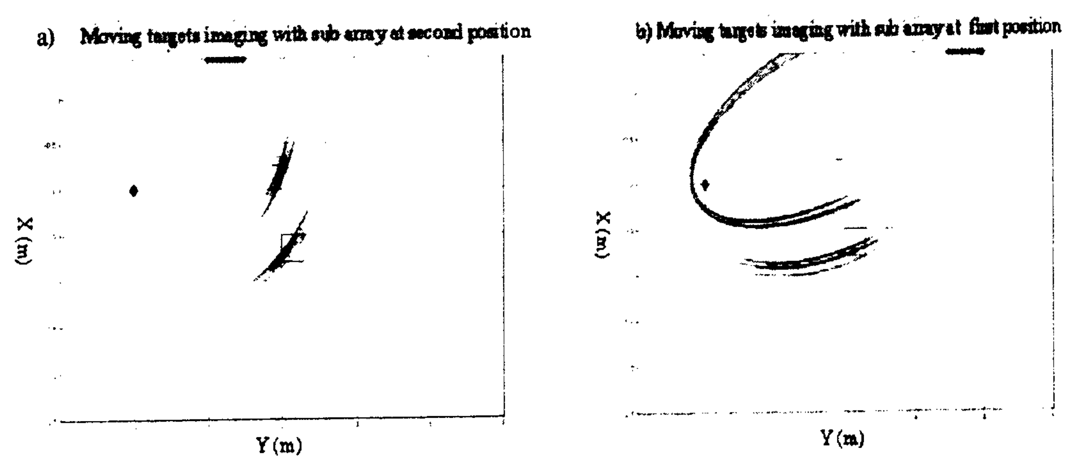

Figure 5. Radar images of moving targets without walls for receiving array position along sidewall

3. 3D THROUGH-WALL IMAGING

This section examines the potential benefit of having 3D through wall imaging capability. The 3D through-wall imaging capabilities of UWB SP radar centered at 2 GHz are first examined, followed by those centered at 10 GHz.

3.1.1. UWB SP centered at 2GHz

The same electromagnetic modeling software is also used to generate simulated data of an UWB SP 2D antenna array in front of a concrete room having a phantom, with and without a rifle. The transmit/receive radar setup is similar to the one described in section 2. However, here the electromagnetic field is recorded every 2 cm on a 2D array in front of the room. Also, the internal dimensions of the room are 3 m wide, 4.5 m long and 3 m high. The target used for the 3D study is a phantom, with and without a rifle, as shown in Figure 6. The position of the phantom inside the room is shown in Figure 7 and its coordinates are given in Table 2.

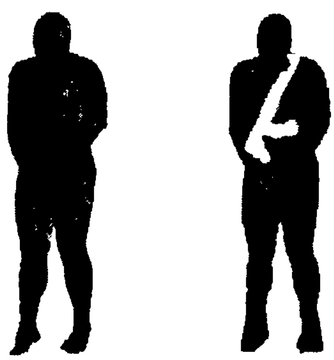

Figure 6. 3D model of phantom with and without rifle

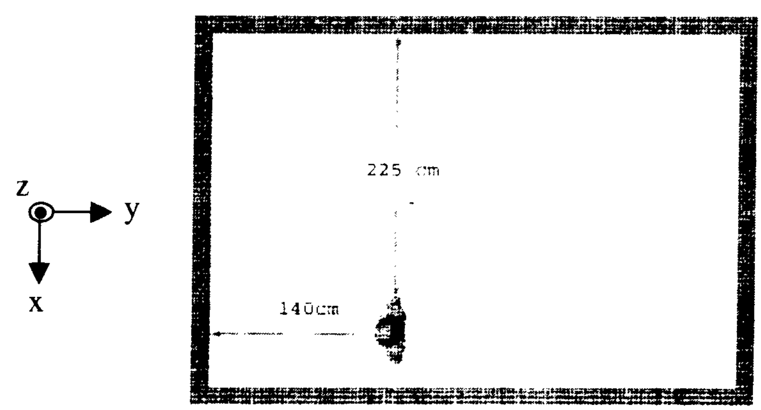

Figure 7. Top view of the phantom inside the concrete room

***Table 2.** Phantom Coordinates for 3D study using UWB SP centre on 2GHz*

Position	Front (cm)	Back (cm)	Side 1 (cm)	Side 2 (cm)	Feet (cm)	Head (cm)
MV_1	y = 166	y = 191	x = 75	x = 133	z = -100	z = 86

The quality and degree of information that can be extracted from radar images is a function of the cross range resolution. In the simulation, the UWB SP signal is transmitted from a single antenna element and received by a receiving array. For the simulated data, the receiver cross range resolution at a given range R is given by [8]:

$$\Delta R_c = \frac{\lambda_0}{D} R \qquad (9)$$

The center frequency of the simulated signal is 2 GHz, which corresponds to a wavelength of 15 cm. Table 3 shows the cross range resolution at a distance of 2 m for different aperture sizes.

***Table 3.** Cross range resolution at a distance of 2m for various antenna aperture sizes*

ΔR_c	Antenna linear size (cm)			
Distance (cm)	**48**	**70**	**100**	**300**
200	62.5	42.9	30	10

We first consider the case where there are no walls since it gives the best images that can be produced for a given array size. It is very difficult to visualize 3D radar data without using 3D visualization tools. This will be done in a future paper, but for now we will only show 2D slices of the 3D radar data along the y-axis. During this study, slices along other plans were examined but the most useful information is obtained using 2D slices along the y-axis.

Figure 8 shows a 2D radar image slice, at y =1.9 m, of the two human phantoms obtained using a receive array 70 cm in width and 48 cm in height. This provides a cross range resolution of about 45 cm in azimuth by 66 cm in elevation at the phantom position. The target images do not appear as a human. There are some differences between the two radar images especially in the area close to the rifle. The only information that can be easily inferred from these 2D images is the width and height of the target images.

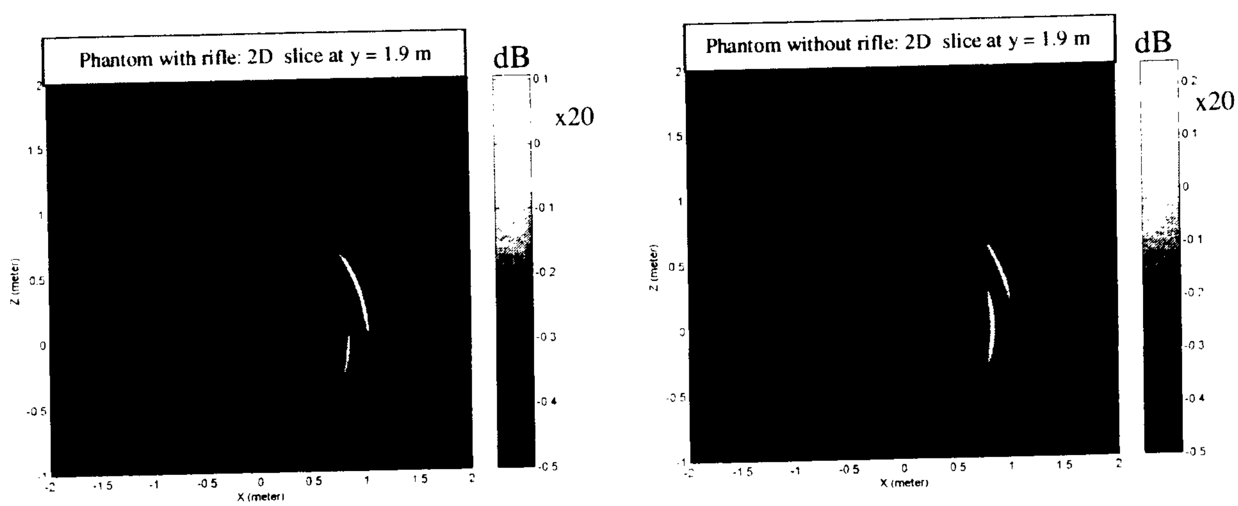

Figure 8. 2D image slice obtained using an aperture size of 70cm by 48 cm (cross range resolution 45 cm by 66 cm).

Figure 9 shows radar images of the same targets obtained using a 3 m by 3 m array, which provides a cross range resolution of 10 cm by 10 cm at the phantom position. We can now identify the targets as standing humans. Although the rifle has been resolved it is difficult to classify it. 3D rendering should significantly enhance the capability to classify the target and identify whether there is a rifle.

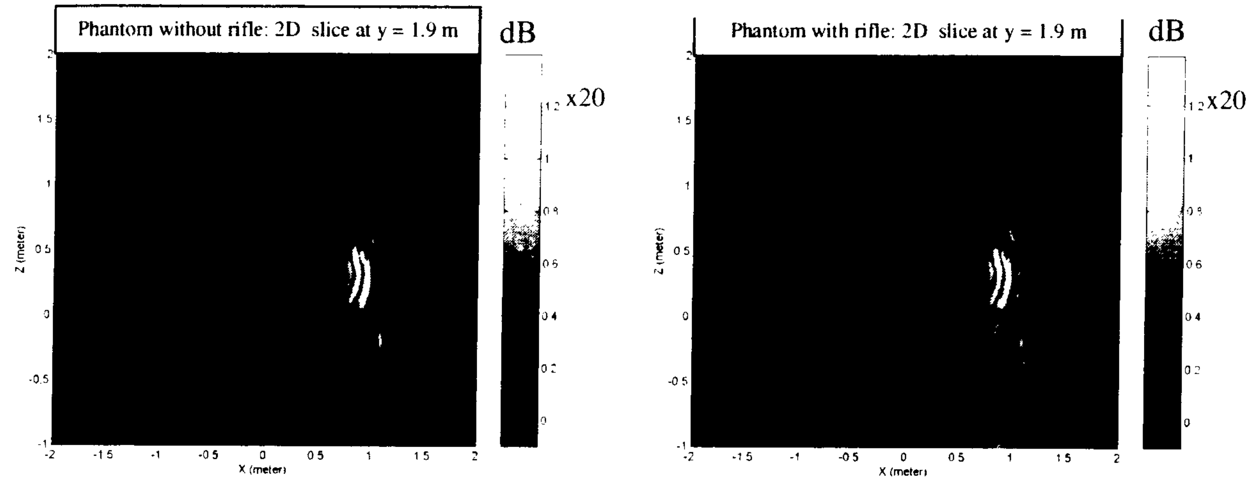

Figure 9. 2D image slice obtained using an aperture size of 3 m by 3 m (cross range resolution 10 cm by 10 cm).

Figure 10 shows radar images of the rifle obtained by subtracting the images of phantom with and without rifle. The presence of the rifle is visible in both cases but it is still difficult to classify the object.

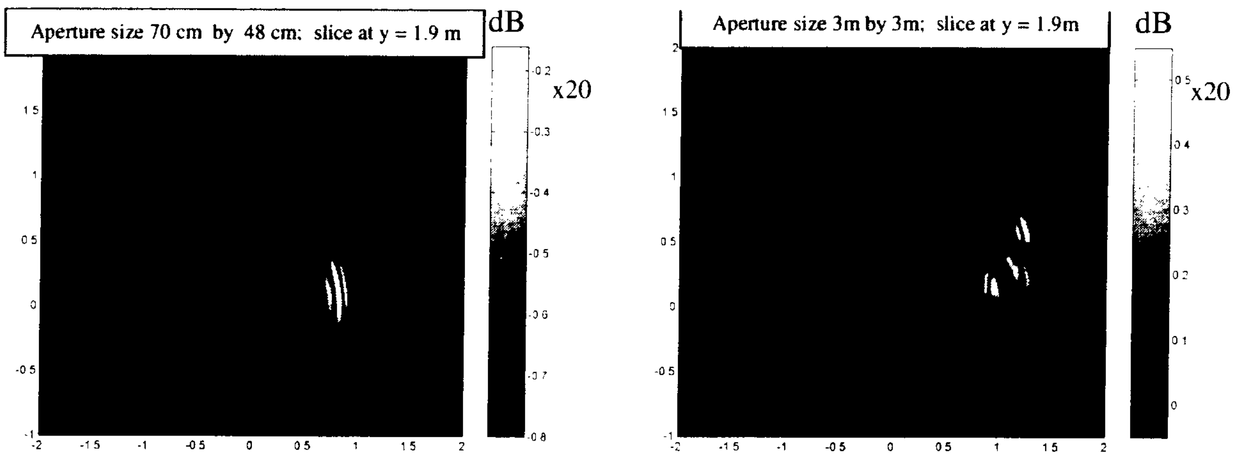

Figure 10. 2D image slice of the rifle obtained by subtracting images of phantom with and without rifle

Figures 11a shows a 2D slice, at y = 2.15 m, of the phantom with the rifle in the concrete room. As expected the target images are displaced from their true positions and the 2D images are defocused. Figures 11b shows the same images when they are corrected for velocity inside the walls. The images are not exactly the same as the "no walls" cases but much better than without correction for the signal velocity. The attenuation due to the concrete wall is approximately 20 dB.

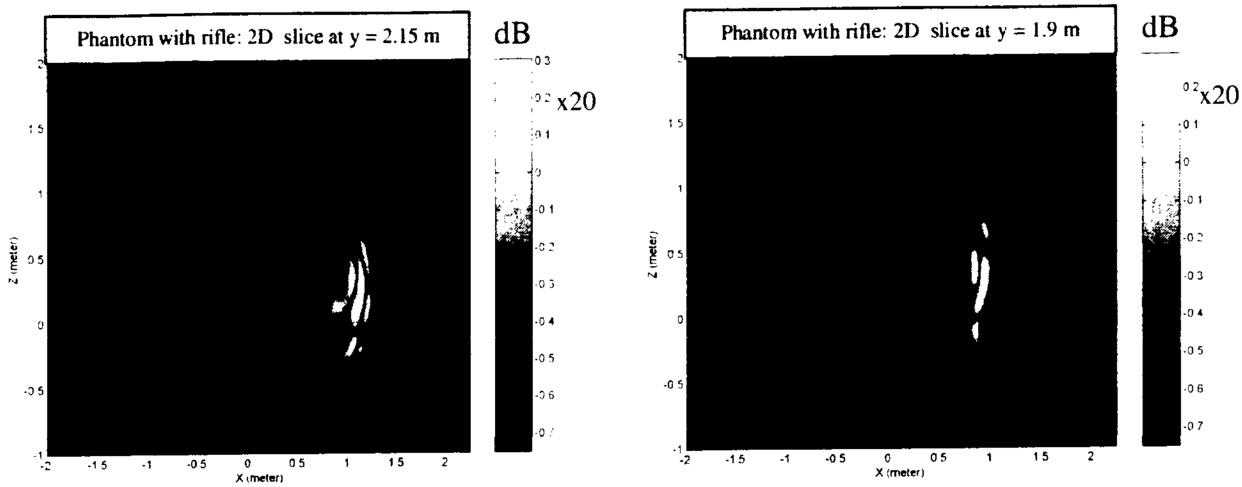

Figures 11a and 11b. 2D image slice of the phantom in presence of the walls: a) without correction and b) with correction

Without using 3D visualization tools, it is extremely difficult to classify a target. Further, a very large receive array (3 m by 3 m) is needed for the simulated 2 GHz UWB SP radar if one wishes to determine target shape. As a result, we have started to investigate the capability of UWB SP radar but centered on 10 GHz.

3.1.2. UWB SP centered at 10GHz

The electromagnetic modeling used in this sub-section is somewhat different and includes only a front wall of 15 cm thickness. The transmitted pulse consists of a half-nanosecond pulse modulated by a 10 GHz carrier. The electromagnetic field is still recorded on a 2D array of receive points facing the front wall with elements spaced at 9 mm. Permittivity is still set at 7 but conductivity is now set to 0.253 S/m compared to 0.05 S/m for the 2 GHz case. The coordinates of the phantom in Figure 6 are given in Table 4.

Table 4. *Phantom Coordinates*

Position	**Front (cm)**	**Back (cm)**	**Side 1 (cm)**	**Side 2 (cm)**	**Feet (cm)**	**Head (cm)**
MV_1	150.3	175.3	-27.35	30.65	-87.3	98.7

We first consider the case where there is no concrete wall. Figure 12 shows 2D slices, at y = 175 cm, of the phantoms obtained with an array of 63 cm in width and 45 cm in height. This aperture size provides a cross range resolution of about 8 cm in azimuth and 11 cm in elevation at that range. Although, there are small differences between the two images, it is impossible to say which one has the rifle. The presence of the rifle is clearly visible when we take the difference between the two images as shown in Figure 13. This approach is very promising for target discrimination, especially when 3D rendering is used.

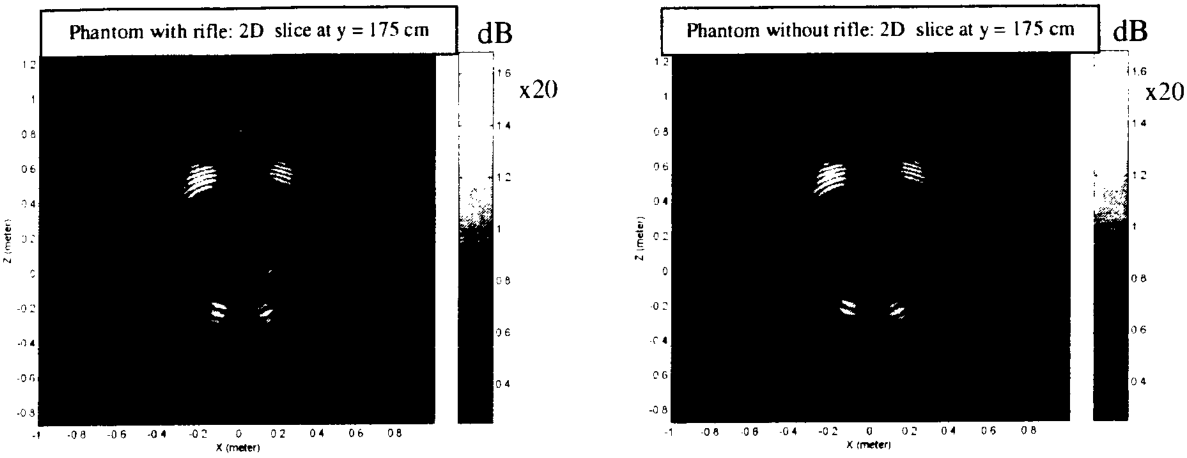

Figure 12. 2D image slice obtained using an aperture size of 63 by 45 cm (cross range resolution 8 cm by 11cm)

Figure 14 shows a 2D slice, at y = 175 cm, of the phantom with the rifle in the presence of the concrete wall (no correction for velocity inside walls). The target image is significantly defocused but the shape of the phantom is still recognizable. The attenuation due to the concrete wall is approximately 70 dB, which is considerable.

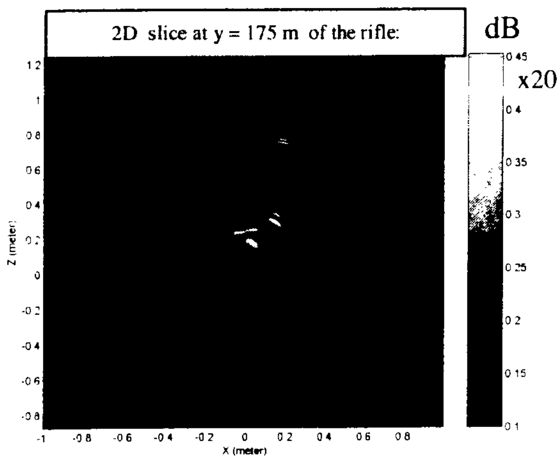

Figure 13. 2D image slice of the rifle at y = 1.75m

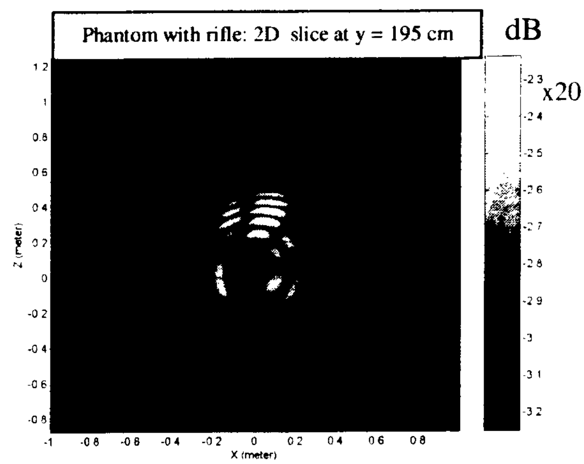

Figure 14. 2D image slice of the phantom with the rifle in the presence of the walls

4. CONCLUSION

This paper shows that UWB SP radar can provide useful surveillance through concrete walls. The radar images show that UWB SP radar can both track the targets moving inside the concrete room and produce static mapping of the room layout including desired targets. This is important since buildings with concrete walls or brick walls are very common throughout the world and the most likely type of environment to be encountered by the law enforcement agencies during operations. The decrease in signal velocity inside concrete wall produces several effects; it defocuses target images and displaces them from their true position. Velocity correction can improve considerably the focusing and quality of the radar images.

UWB SP radar can also be used to conduct multistatic through-wall surveillance. Multistatic through-wall imaging works well as long as the targets are not located in the direct coupling region, i.e., as long as the indirect echo does not interfere with the direct signal.

3D through-wall radar imaging obtained using UWB SP radar centered at 2 GHz requires a very large antenna aperture to be able to see the true shape of human phantoms. The only information that can be easily inferred from these 2D images, using a reasonable size of antenna aperture, is the width and height of the targets. For a similar antenna size, UWB SP radar centered at 10 GHz, can provide better image quality showing clearly the shape of the phantom. Further, 3D rendering of the volumetric radar data will probably allow identification of the target as a human phantom carrying a rifle. Attenuation is much higher at 10GHz, which will make the development of a system a challenging task.

REFERENCES

1. Leblanc, L.J. and Tondreau, J.R., (2003), *Surveillance Requirements for Military Operations in Urban Terrain, Land Force Technical And Staff report*, June 2003
2. *Introduction to Ultra-Wideband Radar Systems*, Edited by James Taylor, CRC Press, 1995
3. A. Taffove and S. Hagness, *The Finite-Difference Time-domain Method*, Artech House, 2000
4. Chamma, W., Kashyap, S., *Detection* of Targets Behind Walls Using Ultra Wideband Short Pulse, Ultra-wideband Short-Pulses Electromagnetics 6, ed by E. Mokole, Plenum Press, 2003, pp493-506
5. Gauthier, S.M. and Chamma, W., *Through-The-Wall Surveillance*, DRDC Ottawa TM 2002-108, 2002
6. Gauthier, S., Chamma, W., et al, *Through-The-Wall Surveillance*, 5th International Military Sensing Symposium, Washington, Dec 2002
7. Lorrain, P. and Corson, D., *Electromagnetic Fields and Waves*, W.H. Freeman and Company, 1970
8. Gauthier S. and Chamma W., *Surveillance Through Concrete Walls*, DRDC Ottawa TM 2003-233, 2003

#522577
CA025049